J Mater Sci (2023) 58:15558–15575

Polymers & biopolymers

Derivatives of linseed oil and camelina oil as monomers for emulsion polymerization

Martin Kolář[1], Jan Honzíček[1], Štěpán Podzimek[1,2], Petr Knotek[3], Martin Hájek[4], Lucie Zárybnická[5], and Jana Machotová[1,*]

[1] *Institute of Chemistry and Technology of Macromolecular Materials, Faculty of Chemical Technology, University of Pardubice, Studentská 573, 532 10 Pardubice, Czech Republic*
[2] *Synpo, a. s., S. K. Neumanna 1316, 532 07 Pardubice, Czech Republic*
[3] *Department of General and Inorganic Chemistry, Faculty of Chemical Technology, University of Pardubice, Studentská 573, 532 10 Pardubice, Czech Republic*
[4] *Department of Physical Chemistry, Faculty of Chemical Technology, University of Pardubice, Studentská 573, 532 10 Pardubice, Czech Republic*
[5] *Institute of Theoretical and Applied Mechanics of the Czech Academy of Sciences, Centre Telč, Prosecká 809/76, 190 00, Prague 9, Czech Republic*

Received: 3 July 2023
Accepted: 16 September 2023
Published online: 13 October 2023

ABSTRACT

Acrylated methyl esters of higher fatty acids derived from camelina oil and linseed oil were synthesized through transesterification, epoxidation, and subsequent acrylation. Methyl methacrylate and butyl acrylate were copolymerized with various amounts of bio-based derivatives (5 – 30 wt% in monomer mixture) to obtain polymeric latexes for coating applications. Successful emulsion polymerizations with up to 25 wt% of the bio-based derivatives were performed with low coagulum (below 2%) and high monomer conversion (around 95%). The incorporation of bio-based derivatives into polymeric latexes was confirmed with infrared spectroscopy. Asymmetric flow field flow fractionation coupled with a multi-angle light scattering was used to analyze the synthesized copolymers in terms of their molar mass distribution. The results revealed that copolymerizing the bio-based derivatives resulted in ultra-high molar mass nanogel fractions formed because of multi-acrylated ingredients derived from polyunsaturated fatty acids. The phenomenon of nanogel formation became more pronounced for the linseed oil-based derivative. Evaluated coating properties showed that latexes comprising the bio-based derivatives provided increased water repellence (about 10° higher water contact angles were achieved for all bio-based coating compositions in contrast to a reference latex). Moreover, latexes comprising chemically modified oils in the content of 25 and 30 wt% provided water whitening-resistant coatings, making the bio-based derivatives promising candidates for replacing petroleum-based monomers in the production of sustainable latex coatings.

Handling Editor: Chris Cornelius.

Address correspondence to E-mail: jana.machotova@upce.cz

https://doi.org/10.1007/s10853-023-08969-4

GRAPHICAL ABSTRACT

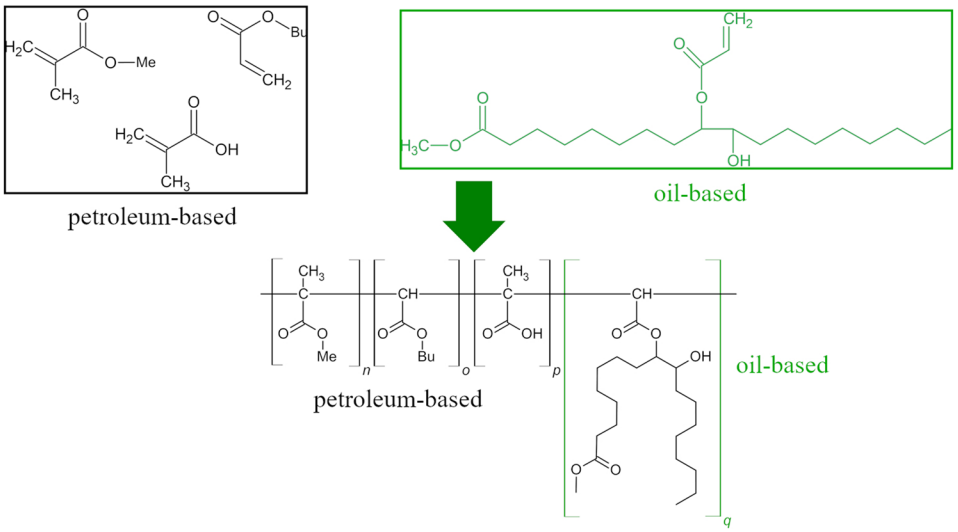

Introduction

Synthetic latexes are manufactured using emulsion polymerization, a process involving a radical polymerization of emulsified unsaturated monomers with low water solubility, initiated using a water-soluble initiator [1–4]. Emulsion polymerization is a widely used technique for a multitude of applications such as surface coating systems (paints, adhesives, sealants) and bulk polymers. The use of water as the dispersion medium is eco-friendly and provides excellent heat dissipation during the polymerization process [5]. A variety of monomers can be used in emulsion polymerization, the most common are esters of acrylic and methacrylic acid, vinyl acetate, or styrene [6]. In recent years, the concerns among scientific and industrial companies about the global depletion of oil feedstock and its negative impacts on the environment evoked new research in the field of renewable resources for the synthesis of polymers [7–13]. These research tendencies also affect the area of emulsion polymerization [14–17].

The use of vegetable oils, i.e., triglycerides of higher fatty acids, has emerged as a promising alternative to fossil fuels due to their abundance, sustainability, and biodegradability. They can be incorporated in their triglyceride form into renewable polymers in a similar way to many ordinary plastics from petroleum chemicals [18–22]. Vegetable oils such as sunflower [23], soybean [24, 25], linseed [26], castor [27], jatropha [28], or rapeseed [29] are widely used for the synthesis of polymers for various applications, e.g., acrylic adhesives [30], alkyd coatings [31], thermo-sensitive films for food conservation [32], and polyurethane composites [25, 27–29]. They have also been utilized as emollients in the cosmetic industry [33]. In addition, vegetable oils can be utilized in the form of esters of higher fatty acids produced by transesterification [34–37]. The esters of higher fatty acids are used mainly as alternative diesel fuel (biodiesel) [38], but they can also represent raw materials for polymer synthesis [31, 39].

Vegetable oils vary especially in the degree of unsaturation of higher fatty acids constituents [40–42]. However, the double bonds present in the fatty acid tails are not sufficiently reactive for common polymerization reactions, necessitating the introduction of more reactive functionalities like acryloyl, hydroxyl, or epoxy groups [43, 44]. Different ways to modify vegetable oils into reactive monomers have been studied, including epoxidation [45–47], hydroxymethylation [48], oxidation [49], and acrylation [50, 51]. Among these approaches, epoxidation followed by acrylation has been often used to introduce acryloyl functional groups via previously attached epoxy groups [39, 52–54].

Utilizing chemically modified vegetable oils in the field of emulsion polymerization remains quite a challenge due to their hydrophobic nature and low solubility in water, which limits their transport and subsequently impedes their incorporation into resulting

polymer particles [55–57]. Despite these difficulties, some successful attempts have been reported. Kaya et al. [58] copolymerized soybean oil-based derivative, containing acryloyl and allylic functionalities with methyl methacrylate. Moreno et al. [59] successfully synthesized film-forming polymers from acrylated linoleic acid. Demchuk et al. [60] prepared stable latexes containing up to 35 wt% of bio-based units in copolymer copolymerizing vinyl derivatives from soybean, sunflower, linseed, and olive oils with methyl methacrylate, styrene, and vinyl acetate. Jensen et al. [61] utilized acrylated methyl oleate in the emulsion polymerization of styrene finding that an increase in bio-based derivative content resulted in a decrease in the glass transition temperature and a higher initiator consumption. Bunker et al. [62] studied emulsion copolymerization of acrylated methyl oleate with acrylic acid revealing the branching of polymer molecules due to chain transfer reactions.

Among the highly unsaturated vegetable oils investigated for use in emulsion polymerization, linseed oil (LO) has become popular [60, 63–66]. It is obtained from the dried, ripened seeds of the flax (*Linum usitatissimum)*. Its molecules are primarily composed of linolenic, linoleic, and oleic acids that can be transformed into functional monomers through grafting of reactive groups [67, 68]. Camelina oil (CO) is another industrially relevant vegetable oil containing a large amount of polyunsaturated fatty acids. This oil is obtained from *Camelina sativa*, which is a cruciferous plant also called false flax [69]. The interest in camelina and its oil has increased in recent years due to its agronomic advantages compared with other traditional oilseed crops, such as the low requirement for fertilizer or water, good adaptivity to unfavorable environmental conditions, and resistance to pests [70]. Camelina is frequently grown as a non-food oilseed crop, avoiding competition with other crops meant for food production [71–74]. It contains about 90% of unsaturated fatty acids with an average of 5.8 double bonds per triglyceride, making CO very attractive for the synthesis of derivates with high functionality [75]. In contrast to LO, CO and its derivatives have hardly been investigated as a raw material for polymer production via emulsion polymerization. To the best of our knowledge, the only information is related to photo-induced emulsion homopolymerization of CO derivative that was functionalized with polymerizable methacrylic groups and hydrophilic polyethylene glycol units, providing self-emulsifiable properties [76].

In our previous work, we demonstrated the successful synthesis of acrylated rapeseed oil-based derivatives and their application in latex protective coatings [52]. In this work, we focused on the synthesis of acrylated derivatives from LO and CO, respectively, and their utilization in emulsion polymerization. The effects of the type and content of the bio-based derivative on the properties of final film-forming latex products, such as colloidal stability, chemical structure, and glass transition temperature, were studied. The application of the bio-based derivatives in the emulsion polymerization process was also evaluated based on the molar mass distribution of the resulting latex copolymers using asymmetric flow field flow fractionation (AF4), coupled with a multi-angle light scattering (MALS) detector. Additionally, coating properties aimed at surface topography and water resistance were tested.

Materials and methods

Materials

The bio-based derivatives were obtained from linseed oil (LO, HB-Lak, Hostivař, Czech Republic), and camelina oil (CO, The National Agricultural and Food Center, Pstruša, Slovak Republic). Their synthesis was performed using the following chemicals purchased from Lach-Ner (Brno, Czech Republic): hydrogen peroxide (30%, technical grade), methanol, potassium hydroxide, sulfuric acid, potassium carbonate, formic acid, hydroquinone, ethyl acetate, and sodium carbonate. In addition, acrylic acid (AA, Sigma-Aldrich, Schnelldorf, Germany) and chromium(III) 2-ethyl hexanoate (ThermoFisher, Kandel, Germany) were utilized for the synthesis of the bio-based derivatives. Methyl methacrylate (MMA), butyl acrylate (BA), and methacrylic acid (MAA), obtained from Sigma-Aldrich (Schnelldorf, Germany), were used as the petroleum-based monomers in all emulsion polymerizations (Supplementary Material Fig. S1). Disponil FES 993 (BASF, Prague, Czech Republic) and ammonium persulfate (Lach-Ner, Brno, Czech Republic) were used as the surfactant and initiator, respectively. 2-Amino-2-methyl-1-propanol (AMP 95, Sigma-Aldrich, Schnelldorf, Germany) was utilized for latex neutralization. All the chemicals were used as received.

Synthesis and characterization of derivatives from vegetable oils

The synthesis of acrylated bio-based derivatives was performed according to a 3-step procedure: (i) The methyl ester of LO (ME_LO) and methyl ester of CO (ME_CO) were obtained by transesterification of the respective vegetable oil, (ii) The epoxidized methyl ester of LO (EME_LO) and epoxidized methyl ester of CO (EME_CO) were synthesized, and (iii) Acrylation of EME_LO and EME_CSO was performed resulting in the acrylated methyl ester of LO (AME_LO) and acrylated methyl ester of CO (AME_CO) [52].

The iodine value and chemical structure were assessed for the synthesized methyl esters, epoxidized methyl esters, and acrylated methyl esters of LO and CO. The iodine value (representing the level of unsaturation) for intermediate and final products was measured according to the Hanus method [77]. The chemical structure of intermediate products and final bio-based derivatives was evaluated using proton nuclear magnetic resonance (^{1}H NMR) spectroscopy and infrared (IR) vibration spectroscopy. ^{1}H NMR spectra were recorded on a Bruker 500 Avance spectrometer (Bruker, Billerica, MA, USA) at 300 K. The samples (50 µL) were dissolved in $CDCl_3$ (1 mL) obtained from Acros Organics. Spectra were referenced internally to residual $CHCl_3$ and reported relative to Me_4Si ($\delta = 0$ ppm). The intensities of the bands were referenced to the methyl ester group (3H). Proportions of different methyl esters of higher fatty acids in intermediate products after transesterification and conversions of the subsequent epoxidation and final functionalization (acrylation) were calculated by using Eqs. (1–5):

$$18:3 = \frac{h(\mathrm{ME})}{h(\mathrm{ME}) + i(\mathrm{ME})} \tag{1}$$

$$18:2 = \frac{c(\mathrm{ME}) - 4 \times 18:3}{2} \tag{2}$$

$$n:1 = \frac{e(\mathrm{ME})}{4} - 18:2 - 18:3 \tag{3}$$

$$n:0 = 1 - n:1 - 18:2 - 18:3$$

$$\alpha(\mathrm{epoxidation}) = \frac{j(\mathrm{EME}) + k(\mathrm{EME})}{a(\mathrm{ME})} \tag{4}$$

$$\alpha(\mathrm{overall}) = \frac{\frac{l(\mathrm{AME}) + m(\mathrm{AME}) + n(\mathrm{AME})}{3}}{\frac{a(\mathrm{ME})}{2}} \tag{5}$$

where 18:3, 18:2, n:1, and n:0 are the proportions of a given methyl ester of higher fatty acid with a specific pattern (no. of carbons: no. of double bonds), and the parameters (small letters) denoted as ME, EME, and AME are the integral intensities of resonances in ^{1}H NMR spectra of a given methyl ester, epoxidized methyl ester, and acrylated methyl ester, respectively.

IR spectra were recorded on a Nicolet iS50 FTIR spectrometer (Thermo Fisher Scientific, Waltham, MA, USA) equipped with a build-in diamond ATR (attenuated total reflection) crystal in the region of 4000–400 cm^{-1} (data spacing = 0.5 cm^{-1}). Raman spectra were recorded on the same spectrometer using the FT-Raman module (Nd:YAG excitation laser, $\lambda = 1064$ nm, power = 0.5 W, data spacing = 2 cm^{-1}) in the region of 4000–200 cm^{-1}.

Synthesis and characterization of latexes

Using the semi-continuous non-seeded emulsion polymerization technique, two sets of latexes were produced. In both sets of latexes, different amounts (5 – 30 wt%) of AME_LO and AME_CO, respectively, were copolymerized with standard petroleum-based monomers (MMA, BA, MAA). A reference latex (REF) was synthesized without any bio-based derivative in parallel. The monomer composition of latex copolymers is shown in Table 1. The latexes were denoted as X_y, where X reflects the vegetable oil type (LO or CO), and y represents the percentage concentration of a given bio-based derivative in the monomer

Table 1 Monomeric composition of latex copolymers differing in the bio-based derivative type and content

Latex name	Bio-based derivative content (wt%)	Monomer (g)			
		MMA	BA	MAA	AME_X[a]
REF	0	21.0	28.0	1	0
X_5[a]	5	19.9	26.6	1	2.5
X_10[a]	10	18.9	25.1	1	5.0
X_15[a]	15	17.8	23.7	1	7.5
X_20[a]	20	16.7	22.3	1	10.0
X_25[a]	25	15.7	20.8	1	12.5
X_30[a]	30	14.6	19.4	1	15.0

[a]X is reflects the vegetable oil type (LO or CO)

mixture. The monomer composition for all the synthesized latexes maintained the MMA/BA ratio of 21/28 (w/w). The procedure and conditions for the synthesis of latexes are described in detail in reference [52]. Each latex type was synthesized twice to verify the reproducibility. The coagulum content and monomer conversion were determined according to standard procedures [78]. The pH of the latexes was adjusted to 8.5 using a 50% aqueous solution of AMP 95.

To evaluate the storage stability of the latexes, differences in the average particle size and zeta potential were detected after storing the latexes at 40 °C for 60 days. The average hydrodynamic diameter and zeta potential values were determined using dynamic light scattering (DLS) with a Litesizer 500 instrument (Anton Paar GmbH, Graz, Austria). The measurements were performed at a solid polymer concentration of 0.01 wt% in the water phase and at a temperature of 25 °C.

The latex copolymers were characterized from the point of view of the molar mass distribution and gel content. The molar mass distribution was obtained from asymmetric flow field flow fractionation (AF4) combined with a multi-angle light scattering (MALS) detector. The experimental setup employed for AF4-MALS was composed of an Agilent 1260 Infinity II chromatograph (Agilent, Santa Clara, CA, USA), equipped with a Wyatt Technology AF4 system Eclipse coupled with a MALS photometer DAWN and an Optilab refractive index (RI) detector. The detectors and software utilized in this study were obtained from Wyatt Technology (Santa Barbara, CA, USA). The separation took place in a long channel of 350 μm thickness using a regenerated cellulose membrane with a molecular weight cutoff of 10 kDa. Tetrahydrofuran (THF) served as the carrier solvent. A linear cross-flow gradient was employed, starting at 2.5 mL min^{-1}, and gradually decreasing to 0.1 mL min^{-1} over a duration of 15 min, followed by 20 min at a flow rate of 0.1 mL min^{-1} and an additional 10 min with zero cross-flow. The channel flow and detector flow were set at 1 and 0.3 mL min^{-1}, respectively. Prior to the analysis, a liquid latex was dissolved (for 48 h) in THF at a concentration of approximately 2.5 mg (solid polymer) mL^{-1}, filtered using a 0.45 μm filter, and then injected in a volume of 100 μL. Data collection and processing were performed using ASTRA 8, while VISION software was used to operate the Eclipse instrument (both from Wyatt Technology). The gel content of latex copolymers was determined according to CSN EN ISO 6427. Around 1 g of a dried polymer film was extracted in THF during 24-h period using a Soxhlet extractor.

Preparation and characterization of latex coatings

A blade applicator was used to apply the liquid latexes onto glass panels, resulting in wet coatings with a thickness of 120 μm. Coalescing agents were not used. After drying at room temperature (RT, 22 ± 1 °C) and 40 ± 5% of relative humidity (RH) for 10 days, the resulting coatings were assessed for their chemical composition, gloss, surface topography, water contact angle (WCA), water whitening, hardness, and glass transition temperature (T_g).

The chemical composition of coatings was detected by IR vibration spectroscopy using the same instrument and experimental condition as stated before. The gloss of coatings, applied on a glass panel sprayed with black matte paint (RAL 9005), was measured according to CSN EN ISO 2813 using a gloss-measuring geometry at 60°. The surface topography of coatings was evaluated employing atomic force microscopy (AFM) using a Dimension Icon (Bruker, Billerica, MA, USA) in PeakForce Quantitative Nanoscale Mechanical mode using ScanAsyst-Air tips (k = 0.4 Nm^{-1}). The topography of the film surface was monitored at a scanning frequency of 0.5 Hz with a resolution of 512 × 512 pixels at areas 10 × 10 and 1 × 1 μm^2, for details see ref. [79]. The roughness was evaluated as RMS value in a similar way as in [80]. The optical microscope Olympus BX 60 was used for macroscopic visualization of the surfaces. WCAs were determined using an optical tensiometer Attension Theta (Biolion Scientific, Espoo, Finland) by applying a 1 μL water drop and measuring the steady-state WCA value at 10 s. Ten measurements were taken for each coating sample at room temperature and 40 ± 5% RH. An objective evaluation of water whitening of coatings cast on glass panels was done by measuring the light transmission, specifically the change in transmittance at a fixed wavelength of 500 nm. A ColorQuest XE Spectrometer (Hunterlab, Reston, VA, USA) was used for this purpose. The coatings were immersed in distilled water at room temperature for 1, 4, and 24 h, and then the transmittance of the exposed coating film area was measured. The extent of water whitening (W in %) was calculated using the following Eq. (6).

$$W = 100 \times \frac{T_0 - T_t}{T_0} \quad (6)$$

where T_0 is the coating transmittance before distilled water exposure, and T_t is the coating transmittance immediately after the immersion test.

The hardness of coatings was tested according to CSN EN ISO 1522 using a Persoz-type pendulum (3034M001 instrument, Elcometer Instruments GmbH, Aalen, Germany). T_g of coating polymers was measured by differential scanning calorimetry (DSC) on a DSC Q2000 instrument (TA Instruments, New Castle, DE, USA) at a heating rate of 10 °C min^{-1} from − 40 to 100 °C. Each coating type was measured twice to verify the reproducibility.

Results and discussion

Characterization of derivatives from vegetable oils

A three-step process was employed to synthesize two derivatives composed of acrylated methyl esters of fatty acids. Initially, transesterification of LO and CO was performed resulting in methyl esters of fatty acids denoted as ME_LO and ME_CO. To obtain epoxidized intermediate products (EME_LO and EME_CO), double bonds in fatty acid tails of ME_LO and ME_CO were epoxidized. Subsequently, the EME_LO and EME_CO were acrylated to obtain acrylated methyl esters of fatty acids AME_LO and AME_CO, respectively. The acrylation process involved the oxirane ring opening and the formation of the acryloyl groups together with the hydroxyl group on the adjacent carbon. The epoxidation and acrylation schemes are portrayed in Supplementary Material Fig. S2.

The degree of unsaturation in the synthesized bio-based derivatives and their intermediate products was also evaluated by their iodine value (Table 2). Epoxidation of ME_LO and ME_CO led to a decrease in the iodine value, although a part of the C=C bonds was found to be intact. The incorporation of acryloyl groups was manifested by an increase in the iodine value. Higher iodine values were detected in the corresponding LO-based products. These findings correlate with the ^{1}H NMR results that revealed a higher degree of unsaturation in the ME_LO in contrast to ME_CO and further verified similar conversions of epoxidation and acrylation reactions in the case of both types of bio-based intermediate products.

^{1}H NMR spectroscopy enabled us to prove the identity of ME_LO (Fig. 1) and estimate the degree of unsaturation. The unsaturation of fatty acid tails is evidenced by a multiplet at 5.41–5.24 ppm (*a*). Methyl ester group gives a characteristic singlet at 3.64 ppm (*b*). All methyl esters are suggested to contribute to the intensity of this signal equally. Its integral intensity implies that the average fatty acid tail contains 2.1 double bonds. Two overlapping triplets (*c*), observed at 2.78 ppm (3 J(1H,1H) = 6.0 Hz) and 2.74 ppm (3 J(1H,1H) = 6.8 Hz), were assigned to bis-allylic methylene groups of polyunsaturated fatty acids 18:3 (4H) and 18:2 (2H), respectively. Methylene groups in α-position relative to the ester function give a well-separated triplet at 2.27 ppm (3 J(1H,1H) = 7.5 Hz; *d*). Mono-allylic methylene groups of 18:1 (4H), 18:2 (4H) and 18:3 (4H) appear as a multiplet at 2.09–1.94 ppm (*e*). Other methylene groups of the fatty acid tails appear as multiplets at 1.65–1.54 ppm (*f*) and 1.36–1.19 ppm (*g*). A well-separated triplet at 0.95 ppm (3 J(1H,1H) = 7.5 Hz; *h*) was assigned to a terminal methyl group of 18:3 (3H). The down-field

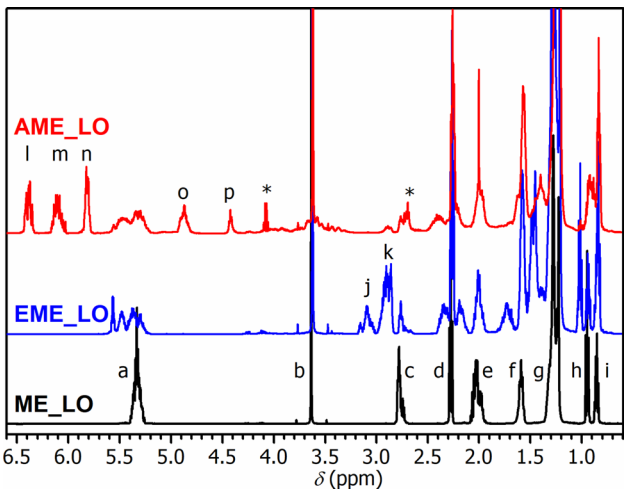

Figure 1 ^{1}H NMR spectra of the LO-based intermediate products and the final LO-based derivative (AME_LO).

Table 2 Iodine values of bio-based intermediate products and final derivatives

Sample	ME_LO	EME_LO	AME_LO	ME_CO	EME_CO	AME_CO
Iodine value (g I_2/100 g)	181.3 ± 4.1	56.4 ± 2.6	76.9 ± 1.9	141.8 ± 3.6	40.0 ± 1.9	65.7 ± 1.1

shift relative to the methyl groups of other fatty acid tails, appearing at 0.88–0.83 ppm (*i*), is due to the proximity of unsaturation. Signals of the ^{1}H NMR spectrum of ME_CO were (Supplementary Material Fig. S3) assigned similarly. The analysis of the spectrum revealed a lower degree of unsaturation (1.7 double bonds per fatty acid tail).

The estimated composition for intermediate products ME_LO and ME_CO (based on the results of ^{1}H NMR spectroscopy) is listed in Table 3. We note that the NMR technique enables to estimate the degree of unsaturation of a given higher fatty acid methyl ester but not the length of the tail. Therefore, the outcome is reported as the sum of methyl esters of saturated fatty acids (*n*:0 = 16:0 + 18:0 + 20:0 + 22:0 + 24:0), the sum of methyl esters of monounsaturated fatty acids (*n*:1 = 18:1 + 20:1 + 22:1 + 24:1), and methyl esters of 18:2 and 18:3 fatty acids.

The epoxidation of ME_LO and ME_CO was followed by IR and Raman spectroscopy. A lower degree of unsaturation in the epoxidized samples EME_LO and EME_CO is well documented by a lower intensity of the C=C stretching band observed in Raman spectra at 1657 cm^{-1} (Fig. 2 and Supplementary Material Fig. S4). ^{1}H NMR spectroscopy enabled to follow the process in more detail. As shown in Figs. 1 and S3, the signals related to unsaturation (*a* and *b*) decreased in intensity and their pattern was changed due to the proximity of epoxy groups. The formation of epoxy functions was unambiguously proven by the appearance of new signals at 3.18–2.82 ppm (*j* and *k*), assigned to CH groups of an epoxy moiety, which well correlates with literature data reported for epoxidized methyl esters of pure fatty acids [81]. The

Table 3 Composition of methyl esters of higher fatty acids in intermediate products ME_LO and ME_CO

Fatty acid pattern (no. of carbons: no. of double bonds)	Content of methyl ester of higher fatty acid (%)	
	ME_LO	ME_CO
n:0[a]	12	13
n:1[b]	16	35
18:2	21	22
18:3	51	30

[a]Sum of methyl esters of saturated fatty acids (16:0 + 18:0 + 20:0 + 22:0 + 24:0)

[b]Sum of methyl esters of monounsaturated fatty acids (18:1 + 20:1 + 22:1 + 24:1)

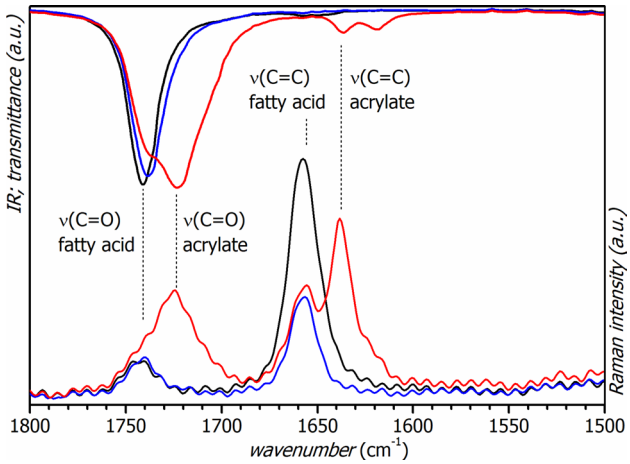

Figure 2 IR and Raman spectra of ME_LO (black), EME_LO (blue), and AME_LO (red).

intensity of signals enabled to quantify the conversion of the epoxidation process. It reached 59 and 68% for EME_LO and EME_CO, respectively. So, in both cases (EME_LO and EME_CSO), the average fatty acid tail contains approximately 0.82 epoxy groups.

As shown in our previous study [52], the acrylation of epoxidized higher fatty acid methyl esters can be verified by IR and Raman spectroscopy. The presence of the C=O stretching band at 1638 cm^{-1} and C=C stretching band at 1724 cm^{-1}, observed in both AME_LO and AME_CO (Fig. 2 and Supplementary Material Fig. S4, respectively), are characteristic for the acryloyl group. ^{1}H NMR spectra of AME_LO and AME_CO show three new multiplets in the region of 6.45–5.75 ppm (*l*, *m*, and *n* in Figs. 1 and S3), those were attributed to the acryloyl function. Signals appearing at 4.87 and 4.43 ppm were assigned to the hydrogen atom of the acrylated fatty acid tail at α-position relative to the acryloyl function. The intensity of the acryloyl signals revealed that the average fatty acid tail in AME_LO and AME_CO contains 0.81 and 0.77 acryloyl functions, respectively. It implies that the overall conversion is 39% for AME_LO and 46% for AME_CO. Similar findings were also presented in the relevant literature related to the acrylation of epoxidized oil-based derivatives. Completely acrylated products were difficult to obtain as some of the epoxy groups remained non-acrylated due to steric hindrance based on the mutual proximity of epoxy groups [36, 82, 83].

Based on the results given above, the bio-based derivatives AME_LO and AME_CO represented a mixture of different methyl esters of higher fatty acids

(predominantly 18:1, 18:2, 18:3, and 20:1 in AME_CO) consisting of fully or partially acrylated compounds that were capable of radical polymerization, but also their non-acrylated counterparts that remained intact in the process of emulsion polymerization. The chemical structures of the most common acrylated derivatives in AME_LO and AME_CO are shown in Supplementary Material Fig. S5.

Characterization of latexes

The properties of the prepared latexes are listed in Table 4. It was found that all the latexes contained a small amount of coagulum that was not affected by the type and content of the incorporated bio-based derivative. A decrease in monomer conversion was found in both sets of latexes with the highest bio-based derivative content (30 wt%). This phenomenon could be caused by poor water solubility of bio-based derivatives [66] and low initiator concentration [61]. Further tests revealed that the amount of incorporated bio-based derivatives did not significantly affect the hydrodynamic diameter of latex particles. Concerning the values of the zeta potential (being negative due to the presence of carboxyl and sulfate groups from copolymerized MAA, persulfate initiator, and adsorbed anionic surfactant, respectively), the increasing amount of copolymerized bio-based derivatives lead to increase in absolute values of the zeta potential, which can be attributed to a partial acid hydrolysis of methyl ester group [84] in the bio-based derivative-building units under polymerization conditions (pH ~ 2) providing carboxyl groups. In addition, the zeta potential values (in absolute terms above − 40 mV) indicate sufficient colloidal stability of all the freshly prepared latexes [85]. After storing at an elevated temperature (40 °C) for a month, no visible settling or creaming, nor any significant increase in the average hydrodynamic diameter occurred, whereas a mild decrease in absolute values of the zeta potential was found, which can be assigned to a desorption of a portion of surfactant molecules from latex particle surface [86, 87]. Nevertheless, the resulting values of the zeta potential after storing proved that all the latexes could be considered long-term stable.

The content of incorporated bio-based building blocks (AME_LO and AME_CO) in the polymer backbone was followed by IR spectroscopy in line with the protocol described previously for fatty acid-modified acrylates [52]. For both sets of latex coatings (differing in the type of the copolymerized bio-based derivative), similar IR spectra for the corresponding concentrations of AME_LO (Fig. 3) and AME_CO (Supplementary Material Fig. S6) in the copolymer were obtained. Figures 3 and S6 document the increasing intensity of CH stretching bands of methylene groups at 2931 and 2855 cm^{-1}, which well correlates with the increasing content of bio-based derivatives used for the synthesis of latexes. This feature verifies successful incorporation of vegetable oil-based building blocks into

Table 4 Properties of latexes in terms of coagulum content, conversion, and storage stability

Latex name	Coagulum content (%)	Conversion (%)	Hydrodynamic diameter (nm)		Zeta potential (mV)	
			Before storing	After storing	Before storing	After storing
REF	1.7 ± 0.6	94.3 ± 1.0	102.1 ± 0.9	104.0 ± 1.6	− 42.2 ± 0.2	− 38.5 ± 1.1
LO_5	0.9 ± 0.2	96.0 ± 1.3	99.3 ± 2.1	96.8 ± 2.5	− 42.4 ± 4.4	− 37.7 ± 2.7
LO_10	1.2 ± 0.43	95.1 ± 1.6	89.1 ± 0.9	90.6 ± 2.4	− 47.0 ± 3.0	− 40.5 ± 3.4
LO_15	1.8 ± 0.3	96.4 ± 1.6	94.0 ± 1.2	95.9 ± 2.1	− 45.2 ± 1.7	− 41.4 ± 0.8
LO_20	1.4 ± 0.3	95.7 ± 0.8	86.4 ± 1.1	87.9 ± 2.3	− 51.7 ± 0.2	− 44.2 ± 1.7
LO_25	1.1 ± 0.2	93.8 ± 0.2	82.2 ± 1.1	82.6 ± 1.0	− 49.5 ± 3.0	− 46.6 ± 2.1
LO_30	1.2 ± 0.1	87.8 ± 0.9	99.9 ± 2.2	100.7 ± 1.2	− 49.7 ± 0.7	− 42.4 ± 0.6
CO_5	0.5 ± 0.2	96.0 ± 0.4	108.2 ± 1.4	109.4 ± 1.6	− 49.7 ± 0.7	− 42.6 ± 0.7
CO_10	1.1 ± 0.2	96.5 ± 1.9	89.0 ± 1.0	89.0 ± 1.5	− 49.9 ± 0.5	− 45.5 ± 1.5
CO_15	1.2 ± 0.4	96.5 ± 0.4	84.1 ± 1.3	85.6 ± 2.0	− 47.7 ± 1.3	− 47.9 ± 2.8
CO_20	1.3 ± 0.2	95.5 ± 1.0	86.0 ± 2.0	86.1 ± 1.3	− 46.6 ± 0.6	− 48.8 ± 2.9
CO_25	0.4 ± 0.1	94.3 ± 0.1	80.1 ± 1.0	80.1 ± 1.8	− 49.3 ± 1.5	− 48.6 ± 3.8
CO_30	2.9 ± 0.4	88.9 ± 0.3	95.0 ± 0.7	96.5 ± 2.1	− 48.4 ± 0.8	− 41.3 ± 0.9

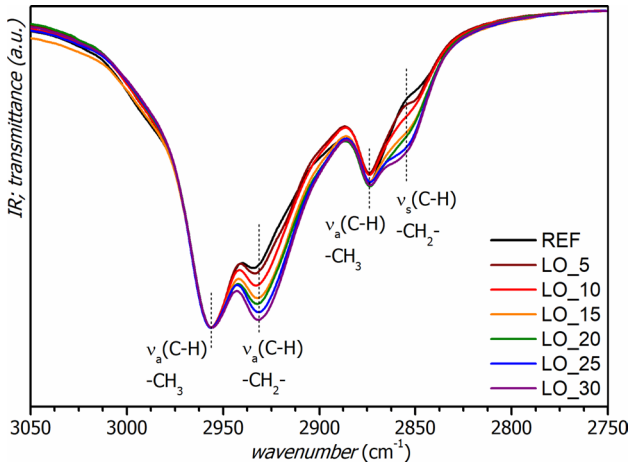

Figure 3 IR spectra of latex coatings differing in the content of the copolymerized LO-based derivative.

the polymer structure. An illustrative structure of a copolymer chain comprising a bio-based building unit is shown in Supplementary Material Fig. S7.

Characterization of molar mass distribution by AF4-MALS

Figure 4 depicts typical RI fractograms and molar mass versus retention time plots for latex copolymers LO_15 and CO_15 (that were synthesized using 15 wt% of the respective bio-based derivative in the initial monomer mixture). The peaks at lower retention times can be assigned to soluble macromolecules, while the peaks at higher retention times belong to cross-linked swollen latex particles (nanogels). Figure 4 also demonstrates a negligible difference between the two investigated bio-based derivatives. All the analyzed copolymers showed similar plots with soluble polymer and nanogel fractions baseline separated. The nanogels were most probably created by cross-linking within the individual latex particles due to the presence of multi-acrylated ingredients derived from polyunsaturated fatty acids. As the molar mass is approximately constant across the nanogel peak, it appears that these species are of very narrow dispersity. Table 5 shows the most relevant characteristics of the two sets of latex copolymers, namely the weight-average molar mass (M_w) and dispersity ($Đ$) of soluble polymer, the weight fractions of soluble polymer and nanogels, and the M_w of nanogels. There is a clear trend of the increasing fraction of nanogels with increasing the concentration of the given bio-based derivative in the monomer feed, which was verified also by determining the gel content (see Table 5).

Characterization of coatings

The evaluated properties of coating films cast on glass panels are listed in Table 6. In terms of appearance, the gloss of coatings gradually decreased with the increasing amount of incorporated bio-based derivatives for both sets of latex coatings. This phenomenon can be caused by the presence of methyl esters of saturated fatty acids, representing a non-negligible fraction in the bio-based derivative batch (see Table 2), as well as by the methyl esters of various unsaturated fatty acids that have not been successfully epoxidized or acrylated (evidenced by ^{1}H NMR analysis and iodine value measurements, see Table 2). Therefore, these ingredients could not participate in polymerization; instead, they could have been sweated out on the

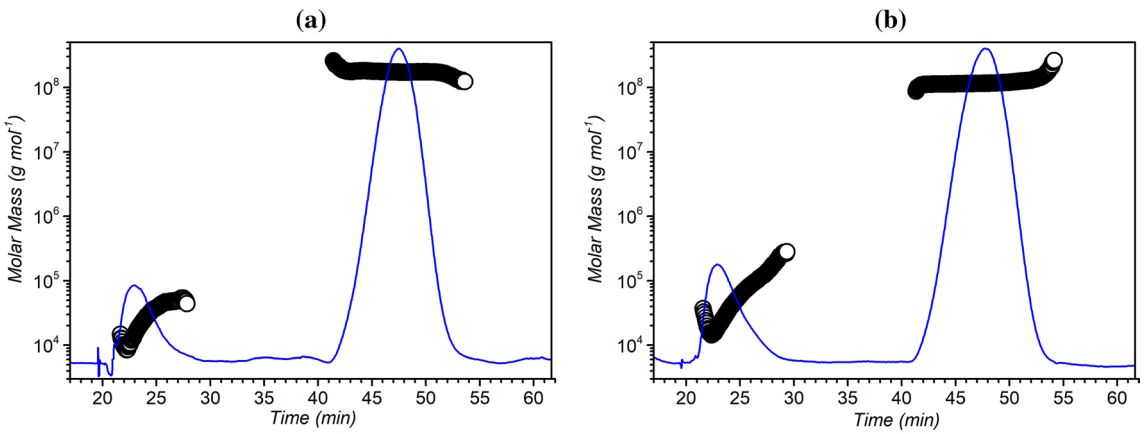

Figure 4 RI fractograms (blue line) and molar mass (black circle) versus retention time plots of copolymers: **a** LO_15, **b** CO_15.

Table 5 AF4-MALS results in terms of M_w, $Đ$, and fractions of polymer and nanogels (the results are averages from two measurements) together with gel content values

Latex name	Soluble polymer			Nanogel		Gel content (wt%)
	M_w[a] (10^3 g mol^{-1})	$Đ$	Fraction (%)	M_w[a] (10^6 g mol^{-1})	Fraction (%)	
REF	6000	36	≅100	–	–	0.98 ± 0.7
LO_5	102	2.11	26.6	128	73.4	71.7 ± 1.3
LO_10	45	1.43	14.7	132	85.3	80.7 ± 1.0
LO_15	33	1.32	13.3	174	86.7	84.1 ± 0.1
LO_20	25	1.27	7.6	145	92.4	88.9 ± 0.6
LO_25	20	1.24	8.6	113	91.4	88.1 ± 0.5
LO_30	15	1.07	5.4	238	94.6	90.9 ± 1.2
CO_5	120	2.86	36.9	218	63.1	67.4 ± 1.5
CO_10	63	2.30	21.1	186	78.9	76.7 ± 2.4
CO_15	48	1.64	15.2	195	84.8	81.7 ± 0.4
CO_20	37	1.47	10.3	207	89.7	85.5 ± 1.3
CO_25	42	1.38	12.4	131	87.6	86.5 ± 1.1
CO_30	28	1.24	9.5	208	90.5	86.8 ± 0.5

[a]The measurement uncertainty was below 10%

'–' The value was not detected

Table 6 Properties of coating films in terms of gloss, WCA, hardness, and T_g

Coating name	Gloss 60° (GU)	WCA (°)	Hardness (%)	T_g (°C)
REF	83.5 ± 0.1	64.9 ± 1.5	5.8 ± 0.2	1.3 ± 0.3
LO_5	83.6 ± 0.2	73.5 ± 2.2	10.7 ± 0.8	3.4 ± 0.7
LO_10	84.1 ± 0.1	74.9 ± 2.7	7.3 ± 0.1	1.5 ± 0.3
LO_15	29.0 ± 0.5	72.4 ± 5.3	7.2 ± 0.4	1.2 ± 1.0
LO_20	27.0 ± 2.6	75.1 ± 2.6	6.1 ± 0.3	−0.6 ± 0.5
LO_25	22.3 ± 1.8	77.1 ± 2.8	5.6 ± 0.2	−3.4 ± 0.6
LO_30	14.9 ± 2.3	66.7 ± 2.7	5.0 ± 0.8	−1.8 ± 0.9
CO_5	54.4 ± 2.2	73.4 ± 5.2	9.0 ± 0.7	3.3 ± 1.0
CO_10	50.8 ± 0.8	73.9 ± 4.0	7.3 ± 0.4	2.4 ± 0.7
CO_15	46.8 ± 1.2	75.6 ± 3.5	7.1 ± 0.4	−0.4 ± 0.8
CO_20	41.4 ± 1.0	76.6 ± 3.8	5.6 ± 0.5	−3.0 ± 0.1
CO_25	34.4 ± 0.1	79.3 ± 1.2	5.1 ± 0.1	−3.9 ± 0.2
CO_30	21.7 ± 0.4	71.0 ± 3.3	4.6 ± 0.3	−2.0 ± 0.2

coating surface during film drying, worsening the surface smoothness. In addition, these substances could also affect the interfacial tension and coalescence of latex particles, resulting in surface roughness.

The surface analysis of a glossy (LO_10) and a matte (LO_30) coating representatives was done by the optical and atomic force microscopes (Fig. 5). From the view of the optical microscopy (top line in Fig. 5), the coating LO_10 was a flat material with a limited no. of surface defects. In comparison, defects (folds and creases), oriented regularly in the form of some facets or grains, were present on the surface of the latex coating LO_30. The size of the facets was in a range of 100–600 µm. In addition, the surface topography was evaluated by AFM to affect the sizes corresponding to the scale of single latex spherical particles. The surface topography revealed a hexagonal array of latex spheres with a relict of the top of original polymer spheres for both coating samples (bottom line in Fig. 5). The waviness of the LO_30 coating surface was verified on a scanned surface of 10 µm^2 (middle line in Fig. 5) and simultaneously reflected in the roughness value of the root mean square (RMS) of 40.8 nm. On the contrary, the coating LO_10 showed a smooth

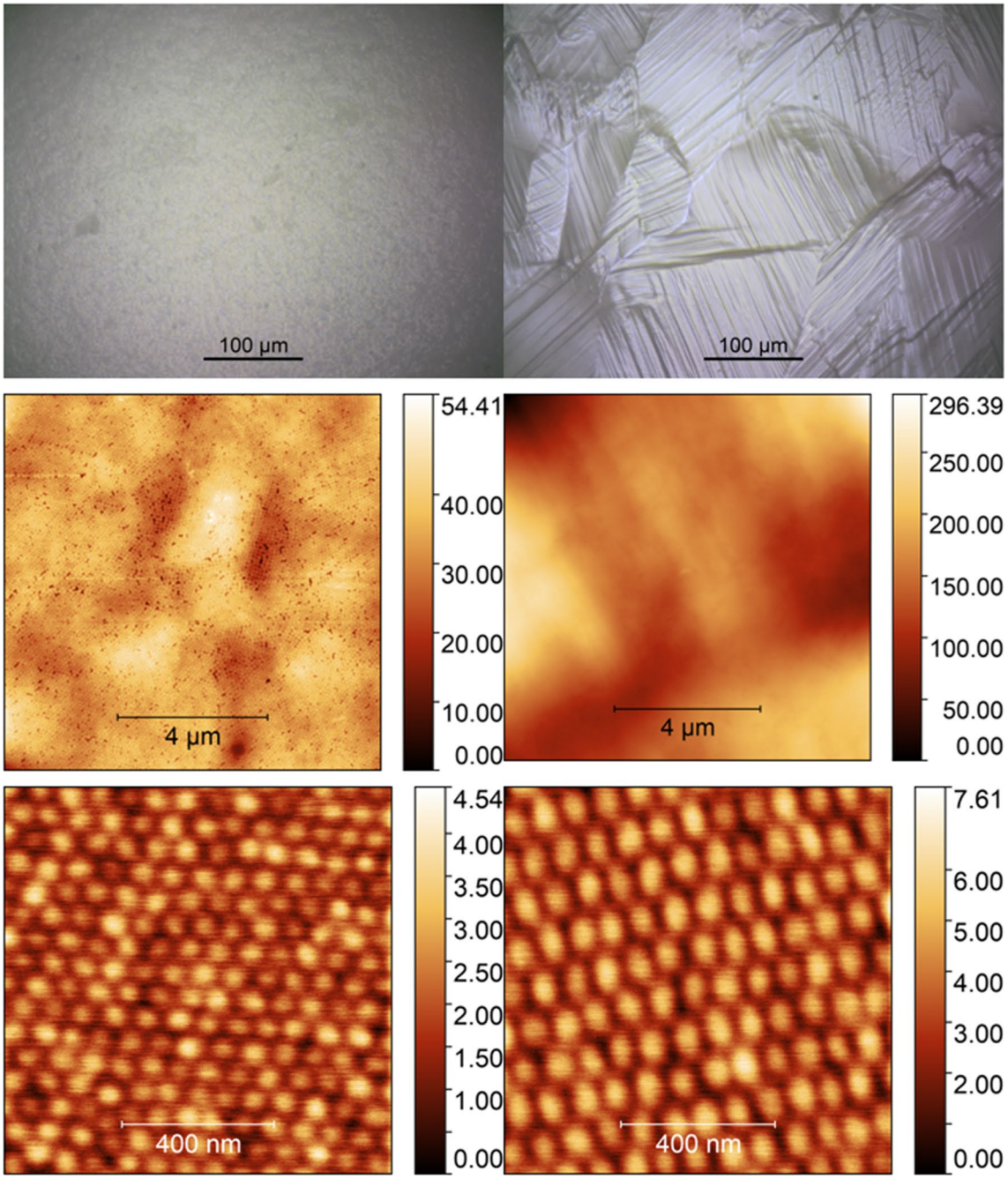

Figure 5 Surfaces and topography of LO_10 (left column) and LO_30 (right column) coatings visualized by optical microscope (top line) and atomic force microscopy (middle and bottom lines).

surface with an RMS of 5.0 nm. Even on a 1 µm scan (bottom line in Fig. 5 and profiles in Fig. 6), we can see differences in terms of the periodicity (distance top-to-top of the spheres relicts) and depth (max-to-min in height), specifically for the LO_10 coating the periodicity and depth differences were 73 and 1.3 nm, respectively, and for the LO_30 coating, these values were higher (103 and 4 nm, respectively). It can be assumed that the loss of coating gloss relates to the macroscopic roughness that resembles a kind of colloidal crystals. The reason may be attributed to the non-polymerizable bio-based ingredients that were excluded in the particle interstices during film-formation or remained adsorbed on individual polymer particles, thereby

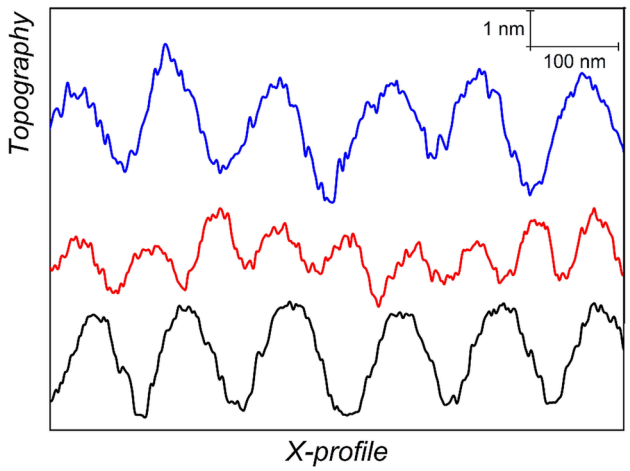

Figure 6 Topographical profiles of REF (black), LO_10 (red), and LO_30 (blue) coatings.

affecting interdiffusion and particle deformation in the coalescence stage or inducing a kind of the self-assembly effect by changes in electrostatic repulsion, and interfacial tension [88].

It was also shown that the incorporation of the bio-based derivatives affected the surface properties of coatings in terms of their wettability. WCA values were in the case of both sets of coatings about 10° higher than for the reference coating (see Table 6). However, no clear relations between WCA increase and the bio-based derivative type or content have been found. The phenomenon of increased water repellence is probably related to the hydrophobic nature of the copolymerized acrylated methyl esters of higher fatty acids. It can also be attributed to the non-polymerized oil-based fractions that could be located on the coating surface. However, the presence of highly hydrophilic hydroxyl groups (originated from epoxy groups) in the copolymerized higher fatty acid tails probably diminished this effect. Finally, the increase in WCA of coatings containing the bio-based derivatives may be associated with their roughness in terms of the nanoscopic surface topography that can be significantly affected by the size of original latex particles. The effect of latex particle size on nanoscopic surface topography of coatings is evidenced in Fig. 6. Latexes REF and LO_30 exhibiting a similar hydrodynamic diameter of polymer particles (approximately 100 nm) provided coatings of analogous topographical profiles in contrast to smoother surface topography of the LO_10 coating made of smaller polymer particles (having the hydrodynamic diameter of approximately 90 nm). The comparison of average hydrodynamic diameters of latex particles (Table 4) with WCA values of corresponding coatings (Table 5) revealed that the smaller the hydrodynamic diameter of polymer particles (the smoother the coating surface at the nanoscopic level), the higher the WCA.

The water sensitivity of the coatings was also tested from the point of view of water whitening. The phenomenon of water whitening, appearing in latex coating films as a consequence of water penetration due to light scattering of water clusters, is a serious and frequently addressed problem of latex protective coatings [89, 90]. As shown in Fig. 7, coatings from latexes synthesized using the bio-based derivatives were less susceptible to water whitening in comparison with the reference latex coating. This effect became more pronounced with the increasing content of incorporated bio-based derivatives of both types, where the latex compositions with the bio-based derivative contents

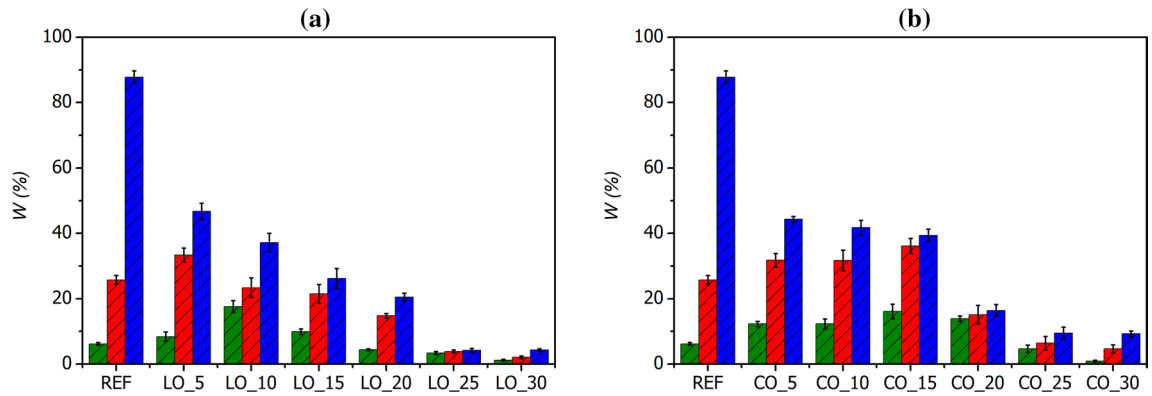

Figure 7 Water whitening of **a** LO-based and **b** CO-based coating films evaluated after 1 (green), 4 (red), and 24 (blue) *h* of water exposure.

of 25 and 30 wt% provided water whitening-resistant coatings. Notably, the LO-based latexes (LO_25 and LO_30) remained transparent to the eye throughout the experiment for up to 24 h, which makes these latexes promising materials for outdoor applications. The explanation of the water whitening phenomenon is usually related to the level of cross-linking of a polymer latex film (the intensity of water whitening is usually inversely proportional to the cross-link density of a latex polymer film; in other words, the more cross-linked film, the smaller water clusters are formed [91, 92]). In this context, the water whitening of the studied coatings is in line with the results of gel content indicating the level of cross-linking inside latex films (Table 5).

In addition, the influence of the bio-based derivative content on the hardness and T_g of coating films was evaluated (Table 6). For both sets of latex coatings, mildly increased hardness and T_g values were determined in the case of incorporating 5 and 10 wt% of the bio-based derivatives, whereas a gradual decrease of these parameters appeared with a further increase in the bio-based derivative content. This behavior seems to show two opposing phenomena: a plasticizing effect of flexible long fatty acid tails in the acrylic polymer backbone, and a hardening effect of cross-linking due to multi-acrylated bio-based ingredients originating from polyunsaturated fatty acid fractions, the latter effect prevailing at higher amounts of incorporated bio-based derivatives. Examples of DSC curves for several coating film representatives are shown in Supplementary Material Figs. S8 – S12.

Conclusions

Camelina oil and linseed oil were chemically modified via transesterification, epoxidation, and subsequent acrylation to obtain acrylated derivatives. These compounds were copolymerized with standard petroleum-based acrylate monomers using the semi-continuous emulsion polymerization to yield two sets of film-forming polymer latexes differing in the bio-based derivative type and content (5 – 30 wt% in the total monomer mixture). For both types of bio-based derivatives, successful emulsion polymerizations with conversions around 95% and coagulum content under 2% were carried out up to 25 wt% of the bio-based derivative in the monomer mixture. In the case of incorporating 30 wt% of the bio-based derivative, a decrease in monomer conversion (below 90%) occurred. It was proved that the incorporation of both types of chemically modified vegetable oils did not affect latex storage stability and resulted in polymers of nanogel character with ultra-high high molar mass (M_w exceeding 10^8 g mol^{-1}). This effect was attributed to the presence of multi-acrylated ingredients derived from polyunsaturated fatty acids and became more pronounced with the increasing bio-based derivative content. The phenomenon of extensive branching and cross-linking was more distinct in the set of polymers synthesized with the linseed oil-based derivative (as linseed oil is richer in linolenic acid). The incorporation of the bio-based derivatives provided enhanced water repellency (10° higher water contact angle in comparison with a reference coating) and a decreased susceptibility to water whitening of latex coatings, where the latexes comprising the linseed oil-based derivative in the content of 25 and 30 wt% provided water whitening-resistant coatings that remained transparent to the eye throughout 24 h-lasting immersion in water. The aspect of sustainability supported by the improved water resistance of coatings makes these latexes suitable candidates for replacing traditional petroleum-based products in the coating industry.

Acknowledgements

We are grateful to the Ministry of Education, Youth and Sports of the Czech Republic, for support through project no. UPA/SG321005. We would also like to thank our colleague Dr. Roman Svoboda for valuable input and assistance.

Author contributions

All authors contributed equally.

Funding

Open access publishing supported by the National Technical Library in Prague.

Data availability

Data will be made available on request.

Declarations

Conflict of interest The authors declare that they have no known competing financial interests or personal relationships that could have appeared to influence the work reported in this paper.

Ethical approval There are no ethical issues involved in this study.

Supplementary Information The online version contains supplementary material available at https://doi.org/10.1007/s10853-023-08969-4.

References

[1] Chern CS (2006) Emulsion polymerization mechanisms and kinetics. Prog Polym Sci 31:443–486. https://doi.org/10.1016/j.progpolymsci.2006.02.001

[2] Thickett SC, Gilbert RG (2007) Emulsion polymerization: state of the art in kinetics and mechanisms. Polymer 48:6965–6991. https://doi.org/10.1016/j.polymer.2007.09.031

[3] Lovell PA, Schork FJ (2020) Fundamentals of emulsion polymerization. Biomacromolecules 21:4396–4441. https://doi.org/10.1021/acs.biomac.0c00769

[4] Li B, Brooks BW (1992) Semi-batch processes for emulsion polymerisation. Polym Int 29:41–46. https://doi.org/10.1002/pi.4990290109

[5] Urban D, Takamura K (2002) Polymer dispersions and their industrial applications. Wiley, Weinheim

[6] Guerrero-Santos R, Saldívar-Guerra E, Bonilla-Cruz J (2013) Free radical polymerization. In: Saldívar-Guerra E, Vivaldo-Lima E (eds) Handbook of polymer synthesis, characterization, and processing. Wiley, Hoboken, NJ, pp 65–83

[7] Satyanarayana KG, Arizaga GGC, Wypych F (2009) Biodegradable composites based on lignocellulosic fibers—an overview. Prog Polym Sci 34:982–1021. https://doi.org/10.1016/j.progpolymsci.2008.12.002

[8] Iman M, Maji TK (2012) Effect of crosslinker and nanoclay on starch and jute fabric based green nanocomposites. Carbohydr Polym 89:290–297. https://doi.org/10.1016/j.carbpol.2012.03.012

[9] Biswas A, Roy M (2015) Green products: an exploratory study on the consumer behaviour in emerging economies of the East. J Clean Prod 87:463–468. https://doi.org/10.1016/j.jclepro.2014.09.075

[10] Lathi P, Mattiasson B (2007) Green approach for the preparation of biodegradable lubricant base stock from epoxidized vegetable oil. Appl Catal B Environ 69:207–212. https://doi.org/10.1016/j.apcatb.2006.06.016

[11] Mandal M, Maji TK (2017) Comparative study on the properties of wood polymer composites based on different modified soybean oils. J Wood Chem Technol 37:124–135. https://doi.org/10.1080/02773813.2016.1253099

[12] de Espinosa LM, Ronda JC, Galià M, Cádiz V (2009) A new route to acrylate oils: crosslinking and properties of acrylate triglycerides from high oleic sunflower oil. J Polym Sci Part A Polym Chem 47:1159–1167. https://doi.org/10.1002/pola.23225

[13] Yao K, Tang C (2013) Controlled polymerization of next-generation renewable monomers and beyond. Macromolecules 46:1689–1712. https://doi.org/10.1021/ma3019574

[14] Derksen JTP, Cuperus FP, Kolster P (1995) Paints and coatings from renewable resources. Ind Crops Prod 3:225–236. https://doi.org/10.1016/0926-6690(94)00039-2

[15] Ladmiral V, Jeannin R, Fernandes Lizarazu K et al (2017) Aromatic biobased polymer latex from cardanol. Eur Polym J 93:785–794. https://doi.org/10.1016/j.eurpolymj.2017.04.003

[16] Lu Y, Xia Y, Larock RC (2011) Surfactant-free core–shell hybrid latexes from soybean oil-based waterborne polyurethanes and poly (styrene-butyl acrylate). Prog Org Coat 71:336–342. https://doi.org/10.1016/j.porgcoat.2011.03.027

[17] Moreno M, Goikoetxea M, Barandiaran MJ (2014) Surfactant-free miniemulsion polymerization of a bio-based oleic acid derivative monomer. Macromol React Eng 8:434–441. https://doi.org/10.1002/mren.201300162

[18] Ragauskas AJ, Williams CK, Davison BH et al (2006) The path forward for biofuels and biomaterials. Science 311:484–489. https://doi.org/10.1126/science.1114736

[19] Mecking S (2004) Nature or petrochemistry?—biologically degradable materials. Angew Chem Int Ed 43:1078–1085. https://doi.org/10.1002/anie.200301655

[20] Williams C, Hillmyer M (2008) Polymers from renewable resources: a perspective for a special issue of polymer reviews. Polym Rev 48:1–10. https://doi.org/10.1080/15583720701834133

[21] Okada M (2002) Chemical syntheses of biodegradable polymers. Prog Polym Sci 27:87–133. https://doi.org/10.1016/S0079-6700(01)00039-9

[22] Gandini A (2010) Monomers and macromonomers from renewable resources. In: Loos K (ed) Biocatalysis in polymer chemistry, 1st edn. Wiley, pp 1–33

[23] Biermann U, Metzger JO, Meier MAR (2010) Acyclic triene metathesis oligo- and polymerization of high oleic sun flower oil. Macromol Chem Phys 211:854–862. https://doi.org/10.1002/macp.200900615

[24] Liu Z, Erhan SZ (2010) Ring-opening polymerization of epoxidized soybean oil. J Am Oil Chem Soc 87:437–444. https://doi.org/10.1007/s11746-009-1514-0

[25] Wu Y, Li K (2018) Acrylated epoxidized soybean oil as a styrene replacement in a dicyclopentadiene-modified unsaturated polyester resin. J Appl Polym Sci 135:46212. https://doi.org/10.1002/app.46212

[26] Wuzella G, Mahendran AR, Müller U et al (2012) Photocrosslinking of an acrylated epoxidized linseed oil: kinetics and its application for optimized wood coatings. J Polym Environ 20:1063–1074. https://doi.org/10.1007/s10924-012-0511-9

[27] Nekhavhambe E, Mukaya HE, Nkazi DB (2019) Development of castor oil–based polymers: a review. J Adv Manuf Process 1:e10030. https://doi.org/10.1002/amp2.10030

[28] Jusoh Taib ER, Abdullah LC, Aung MM et al (2017) Physico-chemical characterisation of epoxy acrylate resin from jatropha seed oil. Pigment Resin Technol 46:485–495. https://doi.org/10.1108/PRT-11-2016-0116

[29] Ho YH, Parthiban A, Thian MC et al (2022) Acrylated biopolymers derived via epoxidation and subsequent acrylation of vegetable oils. Int J Polym Sci 2022:1–12. https://doi.org/10.1155/2022/6210128

[30] Ahn BK, Kraft S, Wang D, Sun XS (2011) Thermally stable, transparent, pressure-sensitive adhesives from epoxidized and dihydroxyl soybean oil. Biomacromolecules 12:1839–1843. https://doi.org/10.1021/bm200188u

[31] Johansson K, Johansson M (2006) A model study on fatty acid methyl esters as reactive diluents in thermally cured coil coating systems. Prog Org Coat 55:382–387. https://doi.org/10.1016/j.porgcoat.2006.02.002

[32] Biddeci G, Cavallaro G, Blasi FD et al (2016) Halloysite nanotubes loaded with peppermint essential oil as filler for functional biopolymer film. Carbohydr Polym 152:548–557. https://doi.org/10.1016/j.carbpol.2016.07.041

[33] Kunik O, Saribekova D, Lazzara G, Cavallaro G (2022) Emulsions based on fatty acid from vegetable oils for cosmetics. Ind Crops Prod 189:115776. https://doi.org/10.1016/j.indcrop.2022.115776

[34] Vávra A, Hájek M, Skopal F (2018) Acceleration and simplification of separation by addition of inorganic acid in biodiesel production. J Clean Prod 192:390–395. https://doi.org/10.1016/j.jclepro.2018.04.242

[35] Hájek M, Vávra A, de Paz CH, Kocík J (2021) The catalysed transformation of vegetable oils or animal fats to biofuels and bio-lubricants: a review. Catalysts 11:1118. https://doi.org/10.3390/catal11091118

[36] Sahoo SK, Khandelwal V, Manik G (2019) Synthesis and characterization of low viscous and highly acrylated epoxidized methyl ester based green adhesives derived from linseed oil. Int J Adhes Adhes 89:174–177. https://doi.org/10.1016/j.ijadhadh.2019.01.007

[37] Vávra A, Hájek M, Kocián D (2021) The influence of vegetable oils composition on separation of transesterification products, especially quality of glycerol. Renew Energy 176:262–268. https://doi.org/10.1016/j.renene.2021.05.050

[38] Kouzu M, Hidaka J (2012) Transesterification of vegetable oil into biodiesel catalyzed by CaO: a review. Fuel 93:1–12. https://doi.org/10.1016/j.fuel.2011.09.015

[39] Ferreira GR, Braquehais JR, da Silva WN, Machado F (2015) Synthesis of soybean oil-based polymer lattices via emulsion polymerization process. Ind Crops Prod 65:14–20. https://doi.org/10.1016/j.indcrop.2014.11.042

[40] Teramoto N (2011) Chapter 2. Synthetic green polymers from renewable monomers. In: Sharma SK, Mudhoo A (eds) Green chemistry series. Royal Society of Chemistry, Cambridge, pp 22–78

[41] Zhang X, Peng X, Zhang SW (2017) Biodegradable medical polymers. In: Zhang X (ed) Science and principles of biodegradable and bioresorbable medical polymers. Woodhead Publishing, Cambridge, pp 1–33

[42] Quirino RL, Kessler MR, Netravali AN, Pastore CM (2015) Vegetable oil-based resins and composites. In: Sustainable composites—Fibers, resins and applications. DEStech Publications

[43] Del Rio E, Galià M, Cádiz V et al (2010) Polymerization of epoxidized vegetable oil derivatives: ionic-coordinative polymerization of methylepoxyoleate: vegetable oil derivatives polymerization. J Polym Sci Part Polym Chem 48:4995–5008. https://doi.org/10.1002/pola.24297

[44] Moreno M, Lampard C, Williams N et al (2015) Eco-paints from bio-based fatty acid derivative latexes. Prog Org Coat 81:101–106. https://doi.org/10.1016/j.porgcoat.2015.01.001

[45] Crivello JV, Narayan R (1992) Epoxidized triglycerides as renewable monomers in photoinitiated cationic polymerization. Chem Mater 4:692–699. https://doi.org/10.1021/cm00021a036

[46] Gandini A, Lacerda TM (2015) From monomers to polymers from renewable resources: recent advances. Prog Polym Sci 48:1–39. https://doi.org/10.1016/j.progpolymsci.2014.11.002

[47] Zhang C, Garrison TF, Madbouly SA, Kessler MR (2017) Recent advances in vegetable oil-based polymers and their composites. Prog Polym Sci 71:91–143. https://doi.org/10.1016/j.progpolymsci.2016.12.009

[48] Eren T, Küsefoğlu SH (2004) Hydroxymethylation and polymerization of plant oil triglycerides. J Appl Polym Sci 91:4037–4046. https://doi.org/10.1002/app.13608

[49] Petrović ZS, Milić J, Xu Y, Cvetković I (2010) A chemical route to high molecular weight vegetable oil-based polyhydroxyalkanoate. Macromolecules 43:4120–4125. https://doi.org/10.1021/ma100294r

[50] Neves JS, Valadares LF, Machado F (2018) Tailoring acrylated soybean oil-containing terpolymers through emulsion polymerization. Colloids Interfaces 2:46. https://doi.org/10.3390/colloids2040046

[51] Khot SN, Lascala JJ, Can E et al (2001) Development and application of triglyceride-based polymers and composites. J Appl Polym Sci 82:703–723. https://doi.org/10.1002/app.1897

[52] Kolář M, Machotová J, Hájek M et al (2023) Application of vegetable oil-based monomers in the synthesis of acrylic latexes via emulsion polymerization. Coatings 13:262. https://doi.org/10.3390/coatings13020262

[53] Habib F, Bajpai M (2011) Synthesis and characterization of acrylated epoxidized soybean oil for UV-cured coatings. Chem Chem Technol 5:317–326. https://doi.org/10.23939/chcht05.03.317

[54] Rana A, Evitts RW (2015) Synthesis and characterization of acrylated epoxidized flaxseed oil for biopolymeric applications. Int Polym Process 30:331–336. https://doi.org/10.3139/217.2961

[55] Laurentino LS, Medeiros AMMS, Machado F et al (2018) Synthesis of a biobased monomer derived from castor oil and copolymerization in aqueous medium. Chem Eng Res Des 137:213–220. https://doi.org/10.1016/j.cherd.2018.07.014

[56] Lu Y, Larock RC (2007) New hybrid latexes from a soybean oil-based waterborne polyurethane and acrylics via emulsion polymerization. Biomacromolecules 8:3108–3114. https://doi.org/10.1021/bm700522z

[57] Quintero C, Delatte D, Diamond K et al (2006) Reaction calorimetry as a tool to determine diffusion of vegetable oil macromonomers in emulsion polymerization. Prog Org Coat 57:202–209. https://doi.org/10.1016/j.porgcoat.2006.08.009

[58] Kaya E, Mendon SK, Delatte D et al (2013) Emulsion copolymerization of vegetable oil macromonomers possessing both acrylic and allylic functionalities. Macromol Symp 324:95–106. https://doi.org/10.1002/masy.201200072

[59] Moreno M, Miranda JI, Goikoetxea M, Barandiaran MJ (2014) Sustainable polymer latexes based on linoleic acid for coatings applications. Prog Org Coat 77:1709–1714. https://doi.org/10.1016/j.porgcoat.2014.05.016

[60] Demchuk Z, Shevchuk O, Tarnavchyk I et al (2016) Free-radical copolymerization behavior of plant-oil-based vinyl monomers and their feasibility in latex synthesis. ACS Omega 1:1374–1382. https://doi.org/10.1021/acsomega.6b00308

[61] Jensen AT, Sayer C, Araújo PHH, Machado F (2014) Emulsion copolymerization of styrene and acrylated methyl oleate. Eur J Lipid Sci Technol 116:37–43. https://doi.org/10.1002/ejlt.201300212

[62] Bunker SP, Wool RP (2002) Synthesis and characterization of monomers and polymers for adhesives from methyl oleate. J Polym Sci Part A Polym Chem 40:451–458. https://doi.org/10.1002/pola.10130

[63] Kohut A, Voronov S, Demchuk Z et al (2020) Non-conventional features of plant oil-based acrylic monomers in emulsion polymerization. Molecules 25:2990. https://doi.org/10.3390/molecules25132990

[64] Booth G, Delatte DE, Thames SF (2007) Incorporation of drying oils into emulsion polymers for use in low-VOC architectural coatings. Ind Crops Prod 25:257–265. https://doi.org/10.1016/j.indcrop.2006.12.004

[65] Kohut A, Demchuk Z, Kingsley K et al (2018) Dual role of methyl-β-cyclodextrin in the emulsion polymerization of highly hydrophobic plant oil-based monomers with various unsaturations. Eur Polym J 108:322–328. https://doi.org/10.1016/j.eurpolymj.2018.09.010

[66] Kingsley K, Shevchuk O, Demchuk Z et al (2017) The features of emulsion copolymerization for plant oil-based vinyl monomers and styrene. Ind Crops Prod 109:274–280. https://doi.org/10.1016/j.indcrop.2017.08.043

[67] Gutiérrez C, Rubilar M, Jara C et al (2010) Flaxseed and flaxseed cake as a source of compounds for food industry. J Soil Sci Plant Nutr 10:454–463. https://doi.org/10.4067/S0718-95162010000200006

[68] Zhao RY, Wang M, Dang ZH, et al (2012) Visual analysis of international oil flax research. In: Wang D (ed) Materials for environmental protection and energy application. Trans Tech Publications Ltd, Switzerland, pp 673–677

[69] Zubr J (1997) Oil-seed crop: *camelina sativa*. Ind Crops Prod 6:113–119. https://doi.org/10.1016/S0926-6690(96)00203-8

[70] Iskandarov U, Kim HJ, Cahoon EB (2014) Camelina: An emerging oilseed platform for advanced biofuels and bio-based materials. In: McCann MC, Buckeridge MS, Carpita NC (eds) Plants and bioenergy. Springer, New York, NY, pp 131–140

[71] Gesch RW (2014) Influence of genotype and sowing date on camelina growth and yield in the north central US. Ind Crops Prod 54:209–215. https://doi.org/10.1016/j.indcrop.2014.01.034

[72] Li Y, Sun XS (2015) Camelina oil derivatives and adhesion properties. Ind Crops Prod 73:73–80. https://doi.org/10.1016/j.indcrop.2015.04.015

[73] Kirkhus B, Lundon AR, Haugen J-E et al (2013) Effects of environmental factors on edible oil quality of organically grown *camelina sativa*. J Agric Food Chem 61:3179–3185. https://doi.org/10.1021/jf304532u

[74] Šípalová M, Lošák T, Hlušek J et al (2011) Fatty acid composition of *camelina sativa* as affected by combined nitrogen and sulphur fertilisation. Afr J Agric Res 6:3919–3923

[75] Kim N, Li Y, Sun XS (2015) Epoxidation of *camelina sativa* oil and peel adhesion properties. Ind Crops Prod 64:1–8. https://doi.org/10.1016/j.indcrop.2014.10.025

[76] Balanuca B, Raluca S, Hanganu A et al (2015) Design of new camelina oil-based hydrophilic monomers for novel polymeric materials. J Am Oil Chem Soc 92:881–891. https://doi.org/10.1007/s11746-015-2654-z

[77] Yildiz Y, Alfeen M, Yildiz B (2019) Determination of iodine value in triisocetyl citrate (Citmol-316) by United States pharmacopeia Hanus method. IJCPS 72:38–41

[78] Ling H, Junyan L (2008) Synthesis, modification and characterization of core–shell fluoroacrylate copolymer latexes. J Fluor Chem 129:590–597. https://doi.org/10.1016/j.jfluchem.2008.04.007

[79] Machotová J, Kalendová A, Voleská M et al (2020) Waterborne hygienic coatings based on self-crosslinking acrylic latex with embedded inorganic nanoparticles: a comparison of nanostructured ZnO and MgO as antibacterial additives. Prog Org Coat 147:105704. https://doi.org/10.1016/j.porgcoat.2020.105704

[80] Smolík J, Knotek P, Schwarz J et al (2021) Laser direct writing into PbO-Ga2O3 glassy system: parameters influencing microlenses formation. Appl Surf Sci 540:148368. https://doi.org/10.1016/j.apsusc.2020.148368

[81] Nameer S, Deltin T, Sundell P-E, Johansson M (2019) Bio-based multifunctional fatty acid methyl esters as reactive diluents in coil coatings. Prog Org Coat 136:105277. https://doi.org/10.1016/j.porgcoat.2019.105277

[82] Grishchuk S, Karger-Kocsis J (2011) Hybrid thermosets from vinyl ester resin and acrylated epoxidized soybean oil (AESO). Express Polym Lett 5:2–11. https://doi.org/10.3144/expresspolymlett.2011.2

[83] Grishchuk S, Karger-Kocsis J (2012) Modification of vinyl ester and vinyl ester–urethane resin-based bulk molding compounds (BMC) with acrylated epoxidized soybean and linseed oils. J Mater Sci 47:3391–3399. https://doi.org/10.1007/s10853-011-6186-0

[84] Šňupárek J Jr, Tuťálková A (1979) Particle coagulation at semicontinuous emulsion polymerization. II. Characterization of surface groups. J Appl Polym Sci 24:915–921. https://doi.org/10.1002/app.1979.070240404

[85] Yilmaz O, Cheaburu CN, Durraccio D et al (2010) Preparation of stable acrylate/montmorillonite nanocomposite latex via in situ batch emulsion polymerization: effect of clay types. Appl Clay Sci 49:288–297. https://doi.org/10.1016/j.clay.2010.06.007

[86] Weng LT, Bertrand P, Stone-Masui JH, Stone WEE (1997) Desorption of emulsifiers from polystyrene latexes studied by various surface techniques: a comparison between XPS, ISS, and static SIMS. Langmuir 13:2943–2952. https://doi.org/10.1021/la962078s

[87] Capek I (2002) Sterically and electrosterically stabilized emulsion polymerization. Kinetics and preparation. Adv Colloid Interface Sci 99:77–162. https://doi.org/10.1016/S0001-8686(02)00005-2

[88] Li Z, Wang J, Song Y (2011) Self-assembly of latex particles for colloidal crystals. Particuology 9:559–565. https://doi.org/10.1016/j.partic.2011.04.006

[89] Khanjani J, Hanifpour A, Pazokifard S, Zohuriaan-Mehr MJ (2020) Waterborne acrylic-styrene/PDMS coatings formulated by different particle sizes of PDMS emulsions for outdoor applications. Prog Org Coat 141:105267. https://doi.org/10.1016/j.porgcoat.2019.105267

[90] Machotová J, Černošková E, Honzíček J, Šňupárek J (2018) Water sensitivity of fluorine-containing polyacrylate latex coatings: effects of crosslinking and ambient drying conditions. Prog Org Coat 120:266–273. https://doi.org/10.1016/j.porgcoat.2018.03.016

[91] Machotova J, Knotek P, Cernoskova E et al (2022) Effect of fluorinated comonomer, polymerizable emulsifier, and

crosslinking on water resistance of latex coatings. Coatings 12:1150. https://doi.org/10.3390/coatings12081150

[92] Machotová J, Kalendová A, Steinerová D et al (2021) Water-resistant latex coatings: tuning of properties by polymerizable surfactant, covalent crosslinking and nano-structured ZnO additive. Coatings 11:347. https://doi.org/10.3390/coatings11030347